Chapter 29
Intrinsic Magnetism in Tin Dioxide

V. Golovanov, N. Ozcan, M. Viitala, T.T. Rantala, and J. Vaara

Abstract Magnetic properties of pure SnO_2 are examined through the first-principles electronic structure calculations based on density functional theory. It is found that the observed ferromagnetism in undoped SnO_2 mainly originates from the bulk double oxygen vacancies.

Keywords Tin dioxide • First principles calculations • Magnetism • Double oxygen vacancy

29.1 Introduction

In search for new generation of spintronic devices the transition metal (TM) doped oxide semiconductors evoked a lot of attention in the past decade with respect to large magnetic moments and room temperature ferromagnetism [1]. After discovering of a giant magnetic moment in Co-doped SnO_2 [2], the various TM-doped

V. Golovanov (✉)
South-Ukrainian National Pedagogical University, Staroportofrankovskaya str., 26, 65008 Odessa, Ukraine
e-mail: alban@te.net.ua

N. Ozcan
Department of Chemistry, University of Helsinki, P.O. Box 55, FIN-00014 Helsinki, Finland

M. Viitala • T.T. Rantala
Tampere University of Technology, P.O. Box 692, FIN-33101 Tampere, Finland

J. Vaara
NMR Research Group, Department of Physics, University of Oulu, P.O. Box 3000, FIN-90014 Oulu, Finland

Y.N. Shunin and A.E. Kiv (eds.), *Nanodevices and Nanomaterials for Ecological Security*, NATO Science for Peace and Security Series B: Physics and Biophysics, DOI 10.1007/978-94-007-4119-5_29,
© Springer Science+Business Media Dordrecht 2012

SnO_2 structures were extensively studied both experimentally [3–6] and theoretically [7–9]. It has been observed that Mn-doped SnO_2 showed very large magnetic moment, at low doping concentration which is far above the spin magnetic moment of Mn [10]. This fact points out on intrinsic defects that can play an important role in mediating of the ferromagnetism in TM-doped SnO_2. Density functional theory (DFT) modeling of TM-doped SnO_2 with presence of oxygen vacancies (V_o) is controversial. In Cr-doped SnO_2 the proximate V_o caused weakening of the ferromagnetic interaction [7], while their presence in Co-doped SnO_2 induces coupling between two Co spins with large Co–Co distance [8]. Furthermore, some authors surprisingly reported that the pure SnO_2 films present magnetic-like behavior at room temperature [11–15]. They assume that lattice defects [11–13] and/or low dimensionality [13, 14] could be the reason of the observed magnetism. However, a consensus on the origin of the magnetism in undoped oxide semiconductor has not yet been reached. Theoretically, first principles calculations [16] showed that neutral cation vacancies in SnO_2 can induce ferromagnetism, provided that concentration of Sn vacancies would be an extremely high. It worth noting that Sn vacancy has high-formation energy, while V_o is easy to form in SnO_2 [17]. Moreover, treatments of SnO_2 films in oxygen atmosphere significantly affect the magnetic ordering [13, 15], which means that oxygen vacancies have obvious impact on the spin polarization of tin oxide.

Recently we have demonstrated [18] that singly ionized oxygen vacancies (V_o^+) can induce local magnetic moments in pure bulk SnO_2, thought according to Wang et al. [19] they couple antiferromagnetically when self-consistent band gap correction (GGA + U_s) is applied. According to numerous calculations [16–21] the V_o^+ defect is unstable with respect to neutral or doubly ionized state at all conditions, which raises the question of the abundance of singly ionized oxygen vacancies in a pure SnO_2 bulk crystal. Anyway, in electron paramagnetic resonance (EPR) studies of tin oxide the resonance at g = 1.89 till recently was widely associated with singly ionized oxygen vacancy [22–24]. Our DFT cluster calculations [18] reassign isotropic g tensor of V_o^+ to a typical for F-center value around 2.00, which corroborates earlier assignments of the corresponding EPR signal observed from SnO_2 [25–27]. In contrast, the strong experimental signal at 1.89 reported in a number of preceding papers, is likely to be caused by some other paramagnetic center, which stimulates a quest for intrinsic defects that can be candidates for a stable magnetic centers in tin oxide. This include double defects, like oxygen vacancy associated with interstitial tin atom (Sn_i + V_o), dioxygen vacancy structures, and various surface arrangements of V_o. Wang et al. [19] reported that Sn_i + V_o defect pair cannot induce ferromagnetism in bulk SnO_2. On the other hand, the EPR measurements [28] revealed four symmetrical resonance lines with g-factor in the range of 1.999–1.89 in gradually reduced SnO_2, where dioxygen vacancies can be readily formed. Therefore, and motivated by the importance to understand the nature of intrinsic magnetism in tin dioxide to the function of any SnO_2 based spintronic device, we generate models of the double oxygen defects in pure SnO_2 bulk and predict their properties using DFT calculations.

29.2 Models and Methods

The computational first-principles density functional (DFT) approach applied here is based on the plane wave basis set and pseudopotential concept to describe electron-ion interaction (CASTEP code) [29]. Utilizing ultrasoft pseudopotentials (USP) [30] the plane wave basis set can be limited considerably [31]. The chosen plane wave cutoff is 380 eV. Oxygen atoms are described by six valence electrons and tin atoms by four plus the corresponding pseudopotential ion cores. Electronic exchange and correlation are included by the Perdew-Burke-Ernzerhof generalized-gradient approximation (GGA) (PBE) allowing possible spin polarization [32]. The Brillouin zone is sampled with $2 \times 1 \times 3$ Monkhorst-Pack *k* points. In separate test calculations the number of k-points was increased to check the convergence. For charged systems, the negative charge of the unit cell is balanced by using constant background charge density. Since such charged model systems can be expected to have the Fermi energy above the conduction band minimum (CBM), occupation numbers were broadened using Gaussian like smearing with a width of 0.1 eV.

A unit cell Sn_4O_8 is chosen for convenience of future modeling of the surface of the crystal instead of the conventional primitive cell Sn_2O_4 with different orientation. This choice will in the future allow us modeling of the most abundant (110) surface using the same orientation in the slab model. The computational supercell is a $2 \times 2 \times 4$ multiple of the chosen unit cell. All structures considered are relaxed while keeping the lattice parameters fixed at optimized from CASTEP values a = 4.899 Å, c = 3.284 Å.

Different methods are used to analyze properties of charged systems, giving qualitatively consistent and complementary results. These methods include; partial density states (PDOS), Mulliken population analysis and distribution of the Kohn–Sham orbitals. Mulliken population analysis gives charges of atoms and bond populations of atom pairs as calculated in terms of density matrix and overlap matrix.

29.3 Results

The possible arrangements of dioxygen vacancies in bulk SnO_2 are denoted in Fig. 29.1, where pairs of oxygen atoms are removed from the octahedron surrounding Sn^{+4} site. Each dioxygen vacancy (except Ovac3 conformation) caused formation of four 5-fold (Sn_{5f}) and one 4-fold (Sn_{4f}) coordinated Sn atoms. Highly symmetrical Ovac3 geometry produces two Sn_{5f} and two Sn_{4f} under-coordinated atoms and does not exhibit spin polarization, while the other configurations in oxidation state +3 induce spin magnetic moments primarily localized on the fourfold Sn atom and first coordination shell of O atoms surrounding the Sn_{4f} with total magnetic moment of 1.02 μ_B per supercell. The spin projected densities show that the unbalanced charge of Sn_{4f} atom spreads toward the empty defect site, while on surrounding oxygen atoms it occupies orbitals orthogonal to direction of

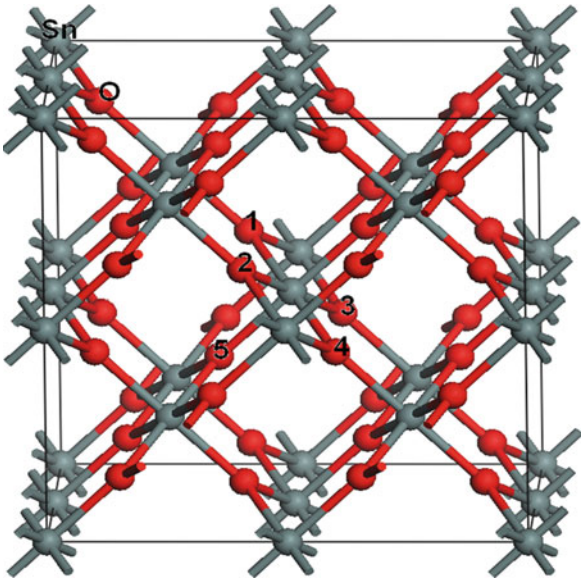

Fig. 29.1 A 48 atom $2 \times 2 \times 2$ supercell of SnO_2 with O-pairs removed from the sites *1* & *3* (Ovac1); *1* & *2* (Ovac2); *1* & *4* (Ovac3) and *1* & *5* (Ovac4). The Sn and O atoms are labeled

the Sn−O bond. Low population of the Sn^{2+}−O bond indicates on prevailing ionic character of interaction between fourfold tin and oxygen atoms.

The key for understanding of magnetic properties in pristine SnO_2 is the dual valency of Sn, which facilitates a reversible transformation of the Sn^{4+} cations into the Sn^{2+} cations. Oxygen deficiency associated with formation of the oxygen divacancies in reduced SnO_2 causes formation of the fourfold bulk Sn atoms. When fourfold coordinated Sn atom is formed, its two 5s-orbitals hybridize with two cation's 5p orbitals forming the two 5s-5p hybrids with strong contribution from the O 2p orbitals of the first coordination shell. These two orbitals along with the remaining 5p orbital of the Sn cation (that also hybridizes with O 2p orbitals) can be seen around the Fermi level in Fig. 29.2, which is representative for all Ovac1,2,4 structures.

Earlier we have demonstrated that such Sn_{4f} atoms able to accumulate a considerable amount of additional charge around itself [31], which results in a lowered dynamical charge with regard to its nominal ionic value Sn^{2+}. When neutral dioxygen vacancy is formed in the bulk of SnO_2, the two electrons compose the lonpair 5s-5p hybrid, while the remaining excess electrons occupy the empty 5s-5p states of the Sn_{4f} ion resulting in a low spin state of the defect.

Removing of one electron from the system results in a weak magnetic moment of only 0.12 μ_B, which points out on the outer compensation of the electron being withdrawn from the 5s-5p orbital of the fourfold coordinated Sn atom.

We have found that the energy level of the 5s-5p hybrid orbitals of the Sn_{4f} cation are located in resonance with the 5s orbitals of the Sn_{5f} atoms, which are also formed around the oxygen divacancy. These orbitals are featured by the excess electron density on their dangling bonds as compared to 5s orbitals of the bulk Sn_{6f}

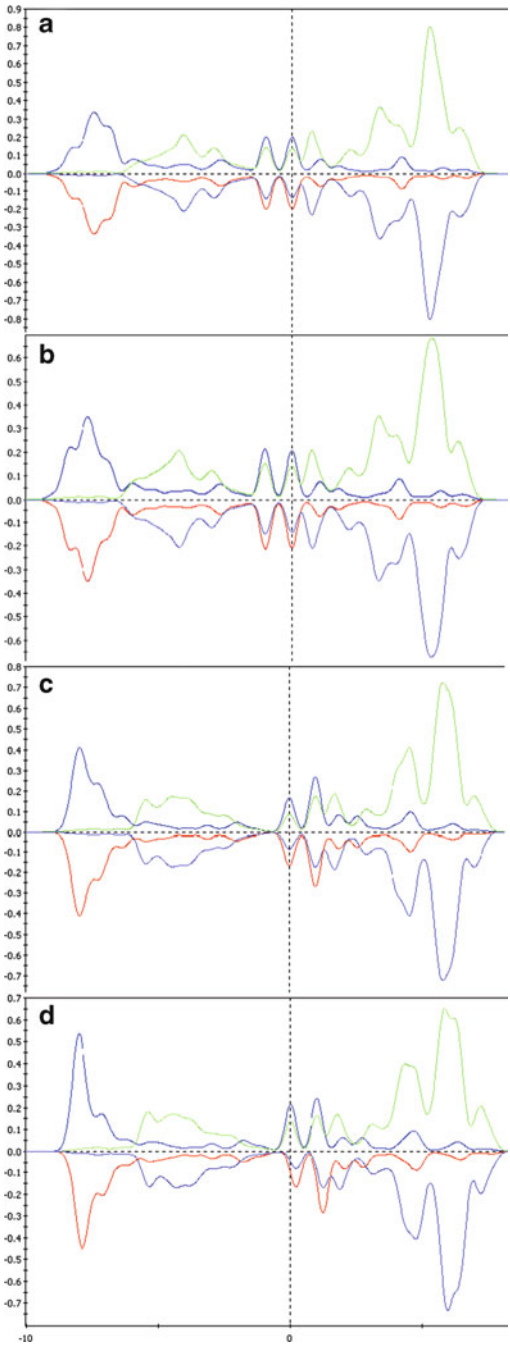

Fig. 29.2 Projective PDOS on the Sn_{4f} for a neutral Ovac4 divacancy (**a**) and Ovac4 structure charged +1 (**b**); +2 (**c**); +3 (**d**). The *dot lines* represent the Fermi level

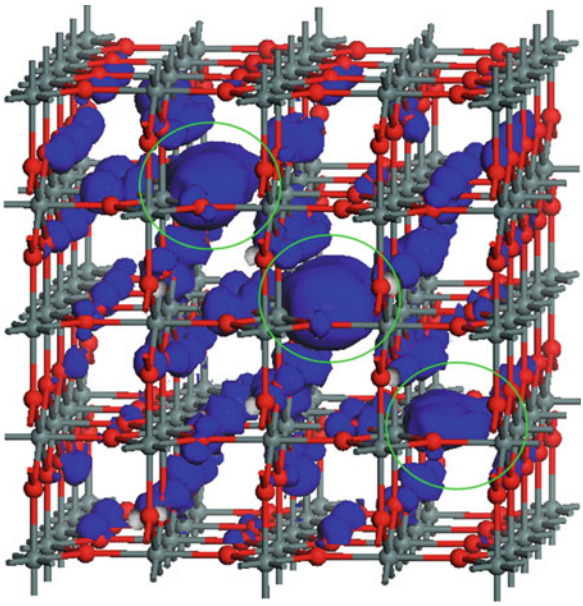

Fig. 29.3 Isosurface of spin density distributions of SnO_2 supercell with three oxygen divacancies (Ovac2) showing their ferromagnetic coupling mediated by oxygen atoms. The energy difference ΔE between AFM and FM ordering ($\Delta E = E_{AFM} - E_{FM}$) is 23 meV

atoms, which is clearly seen from the Mulliken population analysis. Therefore, a partial compensation of the removed electron density to the HOMO orbital of Sn_{4f} atom in case (b) is provided particularly by the under-coordinated Sn_{5f} atoms. However, the situation is changing dramatically when the system undergoes a strong electron deficiency, i.e. dioxygen vacancy is in +3 oxidation state, (Fig. 29.2d). There is no more excess charge at the Sn_{5f} atoms and in order to stabilize its lonepair and preserve its stable Sn^{+2} oxidation state the missing electron density is partially transferred from the nearest O 2p orbitals to the Sn_{4f} cation. The observed spin density demonstrates that Sn_{4f} is not completely occupied as Sn^{2+} ion, which otherwise has an s^2 configuration and a singlet electronic state. At the same time, a hole band is formed by oxygen atoms surrounding the Sn_{4f} cation, which are polarized with the same spin orientation as that of the fourfold Sn atom. These states appear to be ferromagnetically coupled with a rather long-range magnetic interaction, due to strongly Hund's rule coupling and the on-site Coulomb repulsion between the holes in oxygen orbitals [33]. Ferromagnetic coupling between the Sn_{4f} ions in reduced SnO_2 is therefore attributed to the hole-mediated s-p exchange coupling interaction, see Fig. 29.3.

It has been identified by Peng et al. [34] that oxides can be spin-polarized by injecting holes into the host due to large exchange interaction strength of O 2p orbital and quite flat valence band with large effective mass. Since O 2p orbitals are spin split in crystal, the more distant O atoms are also important as they help to overcome the magnetic percolation threshold. Thus ferromagnetism can be realized even at low concentration of Sn_{4f} ions in SnO_2. The total DOS shows that minority spins localized on O 2p orbitals keep the insulating behavior of pure SnO_2 whereas

majority spins are metallic. Such a half-metallic ferromagnetic ground state for the whole system is the promising case for application in spintronic devices. The GGA + *U* test calculations with several *U* values on O-2s orbitals were qualitatively similar to that without *U* and it did not influence the discussion on the magnetism properties of undoped SnO_2.

29.4 Conclusions

We have studied the magnetic and electronic properties of defects in SnO_2 using pseudopotential and method. Our calculations show that bulk SnO_2 is nonmagnetic, but it shows magnetism with a magnetic moment around 1.02 μ_B per one to double oxygen vacancy. The magnetic moment comes mainly from fourfold coordinated Sn atom and O atoms surrounding defect. The ferromagnetic coupling between oxygen divacancies in undoped SnO_2 is attributed to the hole-mediated s-p exchange coupling interaction between the Sn_{4f} cations. The calculations of formation energies show that double oxygen vacancies are stable with respect to single ionized oxygen vacancies. Thus, our calculations demonstrate that the experimentally observed room temperature ferromagnetism in undoped SnO_2 can be attributed to bulk oxygen divacancies in this material.

References

1. Dietl T, Ohno H, Matsukura F, Cibert J, Ferrand D (2000) Zener model description of ferromagnetism in zinc-blende magnetic semiconductors. Science 287:1019–1022
2. Ogale S et al (2003) High temperature ferromagnetism with a giant magnetic moment in transparent Co-doped $SnO_{2-\delta}$. Phys Rev Lett 91:077205
3. Coey J, Douvalis A, Fitzgerald C, Venkatesan M (2004) Ferromagnetism in Fe-doped SnO_2 thin films. Appl Phys Lett 84(8):1332–1334
4. Zhang J, Yun Q, Wang Q (2010) Room temperature ferromagnetism of Ni-doped SnO_2 system. Mod Appl Sci 4(11):124–130
5. Hong N, Sakai J (2005) Ferromagnetic V-doped SnO_2 thin films. Phys B Condens Matter 358 (1–4):265–268
6. Rodrıguez Torres C, Errico L, Golmar F, Navarro A, Cabrera A, Duhalde S, Sanchez F, Weissmann M (2007) The role of the dopant in the magnetism of Fe-doped SnO_2 films. J Magn Magn Mater 316:e219–e222
7. Wei W, Dai Y, Guo M, Zhang Z, Huang B (2010) Effects of oxygen vacancy on the magnetic properties of Cr-doped SnO_2: density functional investigation. J Solid State Chem 183/ 12:3073–3077
8. Wang H, Yan Y, Mohammed Y, Du X, Li K, Jin H (2009) The role of Co impurities and oxygen vacancies in the ferromagnetism of Co- doped SnO_2: GGA and GGA + U studies. J Magn Magn Mater 321:3114–3119
9. Zhang C, Kaob H, Dong J (2009) Origin of ferromagnetism via hole doping in SnO_2: first-principles calculation. Phys Lett A 373:2592–2595

10. Fitzgerald CB et al (2006) Magnetism in dilute magnetic oxide thin films based on SnO_2. Phys Rev B 74:115307
11. Ahmed SA (2010) Room-temperature ferromagnetism in pure and Mn doped SnO_2 powders. Solid State Commun 150:2190–2193
12. Aragon F, Coaquira J, Hidalgo P, Brito S, Gouvea D, Castro R (2010) Experimental study of the structural, microscopy and magnetic properties of Ni doped SnO_2 nanoparticles. J Non Cryst Solid 356:2960–2964
13. Hong N, Poirot N, Sakai J (2008) Ferromagnetism observed in pristine SnO_2 thin films. Phys Rev B 77(3):033205
14. Wang C, Ge M, Jianga J (2010) Magnetic behavior of SnO_2 nanosheets at room temperature. Appl Phys Lett 97:042510
15. Sundaresan A, Bhargavi R, Rangarajan N, Siddesh U, Rao C (2006) Ferromagnetism as a universal feature of nanoparticles of the otherwise nonmagnetic oxides. Phys Rev B 74 (161306):161306(R)
16. Rahman G, Garcia-Suarez V, Hong S (2008) Vacancy-induced magnetism in SnO_2: a density functional study. Phys Rev B 78:184404
17. Kilic C, Zunger A (2002) Origins of coexistence of conductivity and transparency in SnO_2. Phys Rev Lett 88(9):095501
18. Ozcan N, Kortelainen T, Golovanov V, Rantala TT, Vaara J (2010) Electron spin resonance parameters of bulk oxygen vacancy in semiconducting tin dioxide. Phys Rev B 81:235202
19. Wang H, Yan Y, Li K, Du X, Lan Z, Jin H (2010) Role of intrinsic defects in ferromagnetism of SnO_2: first-principles calculations. Phys Status Sol B 247/2:444–448
20. Agoston P, Albe K, Nieminen R, Puska M (2009) Intrinsic *n*-type behavior in transparent conducting oxides: a comparative hybrid-functional study of In_2O_3, SnO_2, and ZnO. Phys Rev Lett 103:245501
21. Singh A, Janotti A, Scheffler M, Van de Walle C (2008) Sources of electrical conductivity in SnO_2. Phys Rev Lett 101:055502
22. Chiodini N, Canevali C, Morazzoni F, Scottia R, Bianchi C (2000) Defect chemistry in ruthenium-supported tin dioxide: a spectromagnetic approach. Int J Inorg Mater 2:355
23. Canevali C et al (2004) Mechanism of sensing NO in argon by nanocrystalline SnO_2: electron paramagnetic resonance, Mossbauer and electrical study. Sens Actuator B 100:228–235
24. Morazzoni F et al (2001) Surface reactivity of nanostructured tin oxide and Pt-doped tin oxide as studied by EPR and XPS spectroscopies. Mater Sci Eng C 15:167–169
25. Ivanovskaya M, Bogdanov P, Faglia G, Nelli P, Sberveglieri G, Taroni A (2001) On the role of catalytic additives in gas sensitivity of SnO_2-Mo based thin film sensors. Sens Actuator B 77:268–274
26. Sun S, Meng G, Zhang G, Gao T, Geng B, Zhang L, Zuo J (2003) Raman scattering study of rutile SnO_2 nanobelts synthesized by thermal evaporation of Sn powders. Chem Phys Lett 376:103–107
27. Popescu D, Herrmann J, Ensuque A, Bozon-Verduraz F (2001) Nanosized tin dioxide: spectroscopic (UV.VIS, NIR, EPR) and electrical conductivity studies. Phys Chem Chem Phys 3:2522
28. Frolova E, Ivanovskaya M (2005) Structural defect formation in inorganic sol-gel derived oxides. Defect Diffus Forum 242–244:143–158
29. Milman V, Winkler B, White JA, Pickard CJ, Payne MC, Akhmatskaya EV, Nobes RH (2000) Electronic structure, properties, and phase stability of inorganic crystals: a pseudopotential plane-wave study. Int J Quantum Chem 77:895–910
30. Vanderbilt D (1990) Soft self-consistent pseudopotentials in a generalized eigenvalue formalism. Phys Rev B 41:7892–7895
31. Maki-Jaskari M, Rantala TT, Golovanov V (2005) Computational study of charge accumulation at SnO_2(110) surface. Surf Sci 577:127–138

32. Perdew JP, Chevary JA, Vosko SH, Jackson KA, Pederson MR, Singh DJ, Fiolhais C (1992) Atoms, molecules, solids, and surfaces: applications of the generalized gradient approximation for exchange and correlation. Phys Rev B 46:6671–6687
33. Elfimov I, Rusydi A, Csiszar S, Hu Z, Hsieh H, Lin H, Chen C, Liang R, Sawatzky G (2007) Nitrogen based magnetic semiconductors. Phys Rev Lett 98:137202
34. Peng H, Xiang H, Wei S, Li S, Xia J, Li J (2009) Origin and enhancement of hole-induced ferromagnetism in first-row d^0 semiconductors. Phys Rev Lett 102:017201